A high efficacy steam soil disinfestation system, Part I: Physical backgrounds and supplying optimization

A high efficiency steam soil disinfestation system, Part I: Physical backgrounds and supplying optimization

P. Gay; P. Piccarolo; D. Ricauda Aimonino; C. Tortia

D.E.I.A.F.A. – Università degli Studi di Torino, 44 Via Leonardo da Vinci, 10095 Grugliasco (TO) – Italy;
Corresponding author: Paolo Gay, Tel. +39 011 6708620, Fax +39 011 6708591, email: paolo.gay@unito.it

Abstract

Steam soil disinfestation is now being reconsidered in open field and greenhouse horticulture for its efficiency in controlling or even eradicating soil borne pathogens, nematodes and weed seeds, while ensuring low ecological impact. Due to the high energetic and labour costs of this treatment, technical solution able to increase the efficiency and to reduce the workload are needed and searched.

This paper represents the design, development and testing of two steam supplying systems for soil disinfestation. Since soil conditions, in terms of texture and humidity, play an important role and significantly influence the efficacy of the treatment, determining the thermal properties of the soil and influencing the steam diffusion, the equipments design followed and extensive laboratory experimentation phase during which the effect on heat efficiency due to soil parameters was assessed. In a companion paper (Gay et al, 2010), a an innovative implement, based on the coupling of the two devices presented in this paper, has been built, connected to a caterpillar track machine, equipped with a steam generator and an automatic guidance system, and used in open field tests.

1. Introduction

Soil disinfestation by steam is an ecological technique used in intensive agriculture to reduce soil borne crop pests before planting high-value crops. Target organisms are pathogenic fungi, bacteria, nematodes and weed seeds that can cause disease or alter production quality.

Steam use for soil disinfestation was envisaged as early as 1888 and was extensively used in the 1960s, but was then substituted by cheaper chemical treatments, mainly methyl bromide.

However, this compound was phased out in 2005 and included in the list of substances responsible for ozone depletion as stated in the Montreal protocol.

As soil steaming is a very effective method, it is considered a valid alternative to methyl bromide for pathogenic fungi eradication as well as for reducing weed emergence. The main drawbacks of steam application are cost and the undesired effect against microarthropods, microorganisms and the natural soil microflora, in particular, nitrifying bacteria which are more sensitive to heat treatments (Fenoglio et al., 2006; Roux-Michollet et al*.,* 2008). In case of prolonged heat exposure, the solubilisation of metal ions could also lead to plant toxicity (Egli et al*.,* 2006).

The most common and simple steam application technique is sheet steaming, which involves covering the soil with a thermo-resistant sheet sealed at the edges, then pumping the steam under the sheet. As steam penetration in the soil is very slow, to ensure sufficient disinfestation at deeper levels, a large amount of steam is required, therefore overheating of the surface layers occur (Van Loenen et al., 2003). Due to the high thermal inertia of the soil, rigid control of the process is difficult and typically leads to excessive and inefficient treatment. To deal with this problem, Dabbene et al. (2003) proposed a model-oriented control algorithm which allows for the reduction of fuel consumption. However, the problems concerning surface overheating and high consumption of fuel and manpower, which heavily influence costs, are not solved.

Other soil steaming techniques that supply steam from under the surface of the soil were developed to reduce energy consumption and labour requirement to lay and seal sheets as well as to improve temperature uniformity into the soil. Hoddesdon pipes or grids of perforated pipes were one the most employed methods for greenhouse soil bed disinfestation in the past. Perforated steel pipes were buried in 30 cm deep trenches and connected to a steam supply source. After the treatment, pipes were pulled out of the soil and reused in the next plot (Lawrence, 1956). Although the method ensured satisfactory disease control, a great deal of labour was required, thus this technique is no longer implemented (Nederpel, 1979).

Spiked grids, also called ‘the comb method’, represented an attempt at labour saving with respect to the previous techniques. The grids consisted of a number of spikes at a distance of about 30 cm, roughly 30 cm long with a set of holes near the tip, connected to pipes. Before treatments, the spikes were introduced into the soil bed while pipes were laid on the surface.

The temperatures achieved in the soil were not substantially higher than those obtained by sheet steaming; in addition, grid positioning still required a considerable amount of labour (Lawrence, 1956; Nederpel, 1979). This technique has recently been applied in nurseries in Holland (Runia, 2000) and in open fields for strawberry and flower production in USA (Gilbert et al., 2009).

Networks of buried drain pipes were widely employed as fixed soil steaming plants in greenhouses. Drain pipes were laid under soil beds at a depth of 50-60 cm spaced out approximately 80 cm from each other. This solution allowed soil tillage to take place in spite of the presence of the pipes and led to a marked improvement with respect to sheet steaming in terms of temperature range achieved by the deeper layer in the soil (Nederpel, 1979; Runia, 1983). However, fuel consumption by the drainage steam system was comparable to that reached by sheet steaming (Runia, 1983). Trials with drain pipe steaming have been carried out in open fields on strawberry and flower crops. In these cases pipe networks have been employed both for steaming and, afterwards, for crop irrigation (Gilbert et al., 2009).

A significant advance in fixed steaming plants was obtained by the introduction of negative pressure steaming (in the 1980s). With this technique, steam is applied from the surface as in sheet steaming, but is forced through the soil by a negative pressure created by a fan that sucks the air out of the soil by means of buried polypropylene perforated pipes. The temperature values achieved at about 45 cm depth are similar (about 60°C after 4 hours of steam application) to those obtained by the drain steam system. Furthermore, using negative pressure steaming, thanks to the significant reduction of treatment times (Runia, 1983), a considerable reduction in fuel consumption (up to 50%) with respect to sheet steaming and drain pipes is obtained.

Improvements, in terms of actual machinery, were achieved by the introduction of metal hoods. Steam is applied to the soil surface beneath the hoods and forced into the soil. This technique is suitable both in greenhouse and in field application, thus a number of self-propelled machines and greenhouse equipment have been developed (see e.g. Pinel et al., 2000; Gay et al., 2010, and references therein). Although reasonable efficiency and a significant reduction of the workload have been achieved, the temperature of the deeper layers that are used by the crop roots could be inadequate to control resistant pathogens, especially if compared with sheet steaming (Pinel et al., 2000).

Different kinds of steaming ploughs, rakes and blades have been developed since the 1950s. With these systems steam was applied up to a 40 cm depth while a winch slowly pulled the implement through the soil bed. The distribution of temperature was rather uniform, but strongly variable with changes in the winch pulling speed (Nederpel, 1979, Bartok, 1994).
The technique of sub-surface steam injection has recently gained an increasing importance in many applications, for example in the field of environmental engineering where it is used for the distribution or remediation of contaminants in the soil or in chemical engineering where is used for rapid heating of porous media, for filtration processes and mechanical/thermal dewatering (see e.g. Miller *et al*, 1998, for an extensive overview).
Whatever technique is adopted, the performances of soil steaming, expressed as temperature persistence and heating efficiency, are highly influenced by soil texture and humidity (Runia, 1983, and Minuto et al., 2005).

This paper presents the design and testing of efficient steam supplying devices, evaluating the effect of different soils and different moisture levels on the heating performances. These results have led, in the companion paper (Gay et al., 2010), to the development of a steam supplying implement to be connected to a non-conventional soil disinfestation machine, which allows the treatment of extended surfaces without assistance by human operators. In particular, this solution relied on the combining of the steam injectors and the hood developed in this paper.
The paper is written as follows: Section 2 introduces the physical backgrounds and constraints of the heating process of the soil; Section 3 describes the adopted experimental set up, constituted by a laboratory-scale pilot plant, a 3D temperature measuring system and a generator of superheated steam, and reports the experimental design. In Section 4 the experimentation results concerning the performances of different steam supplying techniques in combination with different type of soils, at different moisture levels are presented and discussed. Finally, conclusions are drawn in Section 5.

2. Background

As agricultural soil is an unsaturated moist porous medium, modelling heat transport is complicated by the great variability of soil properties (e.g. physical structure, moisture level,

organic matter percentage) as well as by the thermal behaviour that is governed both by heat and mass transfer (Balghouthi et al., 2005). Heat flux through soil is influenced by the thermal properties of the solid phase and by the complex system of hydraulic and water vapour driving forces and heat exchanges among the solid, liquid and water vapour phases which involve condensation, evaporation, convection and diffusion phenomena.

A steam treatment breaks the natural thermal equilibrium of soil forcing a multiphase high temperature flow through its pores quickly enhancing soil temperature.

For soil disinfestation, two ways to supply steam are typically adopted: on surface or in depth. Surface and deep steam supplying differ for the orientation of the resulting flows with respect to gravity. Surface steam treatment has been described as a one-dimensional flow in a vertical column of soil; some numerical models simulating this phenomenon were developed (Bergins et al., 2005; Brouwers, 1996; Miller et al., 1998; Crone et al., 2002). From these theories, four different regions, as reported in Fig.1, can be highlighted. The first surface layer is filled by superheated steam (upstream region), followed by a two-phase zone characterized by the joint presence of liquid and vapour phases, where both evaporation of the immobile water and condensation occur (two-phase region). Then, saturation progressively increases until a condensation front is formed. This is the boundary to the following liquid region, where the soil is completely saturated. Here the temperature decreases quickly and the heat is slowly transferred by conduction through the liquid phase. Finally, there is a downstream region filled by inert gas at ambient temperature.

The condensate flows off downwards in a plug flow and replaces the gas that initially filled the soil porosity. The condensation front moves in the same direction with a speed that is typically three magnitudes of order less than the speed of the steam itself. Since condensation water tends to seal soil porosity, the liquid region increases in thickness and the steam penetration, in terms of condensation front speed, progressively slows down in deeper layers (Hanamura & Kaviany, 1995). In the case of steam supplied by a constant pressure source, the inlet steam flow rate decreases as the elapsed time increases and condensate is formed within the soil.

Instead, in the case of deep steam injection, steam naturally moves upwards, towards the surface, establishing a mixed liquid/vapour rising flow. In particular, the steam supplied by an injector forces the re-evaporation of condensate that contributes to deplete soil porosity,

facilitating steam diffusion. The remaining part of condensate water slowly percolates in the deeper layer of soil in a descending flow. This reiterated partial re-evaporation and re-condensation constitutes a heat pipe type mechanism that allows the achievement of a high heat transfer rate during the steam supply phase. Finally, a steep temperature gradient can be observed in the thin layer of soil close to the surface: in this region the dominant heat transfer factor is conduction.

In soil steaming practice, a great part of the steam is lost in the atmosphere through cracks and fissures that are created e.g. by the chassis of the injector device. This can be critical when the injection device (e.g. a perforated bar) is continuously dragged. To reduce these steam losses, and maintain the heat in the soil as much as possible, in many cases plastic mulching is applied after the treatment.

This type of heat transfer is similar to the "steaming ground" phenomenon, which has been thoroughly analyzed and studied when describing thermal manifestations (mainly steam flux) from the upper part of a geothermal reservoir or volcanic-hydrothermal reservoir (Hochstein & Bromley, 2005; Iwamura & Kaneshima, 2005).

In the case of steam injection oriented perpendicular to gravity, two orthogonal one-dimensional flows are combined. Shoda et al. (1998) proposed two-dimensional simulations which showed time-wise evolutions of the steam front, temperature and liquid and vapour fields occurring in constant pressure steam injection processes to restore groundwater aquifers contaminated by non-aqueous phase liquids such as hydrocarbon fuels.

The thermal behaviour of the soil depends on the specific heat transport mechanisms that are involved or forced by machines and tools used for disinfestation and on the condition, physical structure and its moisture content, of the soil.

3. Materials and Methods

On the basis of the reported theoretical backgrounds on thermo physical properties of steam/soil mixtures, two steam distribution devices have been developed and compared to the classic sheet steaming method. The influence of soil texture and water content was assessed on two different types of soil, representative of horticultural soils in northwest Italy, at three different moisture levels.

3.1. *Steam distribution systems*

Two different small scale prototypes for steam application were tested:

- A square hood diffusion system formed by an iron hood (200 x 0.3 mm) surrounded by a 30 mm welded iron flange, which, during the treatment, remained partially buried to reduce steam leakages. Steam diffused under the hood through four 1 mm holes.
- An injector for steam distribution directly under the soil surface, consisting of a 250 mm long and 21 mm of diameter zinc-coated steel tube with a sharp tip. Steam was supplied by a 2.5 mm diameter hole located 20mm from the tip. A stop-collar bolted to the injector regulated the depth of the hole at 120 mm in the soil.

Both steam diffusers were tested and compared to the traditional sheet steaming technique. Sheet steaming trials were carried out covering the soil with a plastic film while steam was distributed with a diffuser developed to simulate the holed pipe normally employed in open field treatments. This diffuser was implemented with a 21 mm diameter, 70 mm length, zinc-coated steel tube with a sealed end, and sixteen 1 mm holes distributed on its lateral surface.

3.2. *Steam generator and pilot plant*

In order to operate under controlled conditions, a laboratory pilot electrical steam generator was connected to the distribution systems under test, which supplied steam to soils with predetermined characteristics contained in a plastic trial box (400 x 400 x 400 mm) equipped with a three dimensional temperature probe (Fig. 2).

The steam generator, of a nominal thermal duty of 8500 W, supplied up to 4 kg/h of steam at an adjustable pressure by a pressure switch, ranging from 50 kPa to 400 kPa of relative pressure. To reduce condensation, steam was superheated by an electrical 1600W heater. The steam flow was regulated through a manual ball valve and measured by a rotameter positioned upon the generator output. After the defined treatment time, the steam flow was stopped by a solenoid valve, as shown in the scheme of Fig. 2.

The temperature probe was designed for the evaluation of the time-space temperature distribution in the soil during and after steam supply with the three different techniques considered in the paper. The probe consisted of three superposed square grids (150x150 mm)

buried in the soil at 30 mm, 90 mm and 150 mm depth. Each grid was equipped with 16 thermocouples 50 mm spaced on the grids, constituting a three-dimensional matrix of 48 sampling points. The temperature probe monitored a soil volume of 150 x 150 x120 mm located in the centre of the plastic box avoiding, as much as possible, border effects. The frame of the probe was entirely built with thin balsa wood coated by epoxy resin, in order to avoid thermal coupling phenomena that could compromise measurements.

Temperature data were acquired every 5 seconds by means of a 48 inputs National Instruments Field Point 2000® data logger and stored on a PC, which also controlled the solenoid valve by a digital I/O interface. Data acquisition and steam supply control were managed contemporarily by software developed for this purpose using Labview®.

The raw data acquired by the matrix probe were interpolated using Matlab® by a 3D spline (Wahba, 1990) to obtain a three-dimensional spatial distribution of the temperature inside the bulk of the soil. The assessment of soil heating was carried out analyzing the 3D time evolution of the temperature as well as the mean temperature calculated, for each time instant, on the data acquired by the sensors on each layer of the probe.

3.3. *Experimental design*

Soils were collected in two horticultural farms in the northwest of Italy. In particular, soil A (sandy-loam) was collected in Albenga (44°04'01" N, 8°12'45" E; Ligurian region), while soil B (sandy) came from a farm near Turin (44°59'47" N, 7°43'29" E; Piemont region).

The characteristics of the two soils are summarized in Table 1. Soil moisture content was expressed as fraction of its Field Capacity (FC). Three moisture levels were chosen at 40%, 60% and 80% of the FC, which correspond to the absolute moisture contents reported in Table 2.

Soil texture was determined with the Bouyoucos hydrometer technique, while the FC was estimated according to the Richards plates' method (Cavazza, 1981).

For each combination of steam distribution system, soil type and moisture content level, three repetitions were performed for a total of 54 trials.

3.4. *Measurement procedure and test conditions*

Particular care was dedicated to the experimental procedure in order to operate in well defined and homogeneous conditions, in particular for what concerned soil features. For this reason, before analysis and trials, the two soils were sifted through a 5 mm sieve to prevent undesired effects due to the presence of stones and lumps. Although this situation does not represent real field conditions, where the texture is much more irregular, this operation is essential to guarantee the same experimental conditions in the different trials. However, this condition approximates the average situation of the field as, in actual practice, before any sort of disinfestation treatment, soil is generally well tilled as it is prepared for seeding. Before each set of trials, the soil was prepared at the desired level of moisture content according to the procedure described in Gay et al. (2008) and Ricauda (2008).

Lots of about 200 kg of sifted soil were obtained from each soil type and used on sets of three trials. Each soil lot was weighed then put into a concrete mixer where the proper quantity of water was added to reach the desired moisture content by a manual fog nozzle.

Soil was then coarse sifted with a 10 mm square grid in order to break up lumps formed during the mixing phase. As a short storage period was needed between trials, the prepared soil was kept in three identical plastic boxes covered with a plastic film to avoid water evaporation. Before sealing the storage boxes, three samples of soil were taken with a 100 cm^3 stainless steel cylinder with the aim verifying the final moisture content using the gravimetric method.

Soil water content (M) was expressed as percentage of wet soil weight using the following equation (Cavazza, 1981):

$$M = \frac{m_w - m_d}{m_w} \cdot 100 \qquad (1)$$

where m_w and m_d are the masses of wet and dry soil respectively.

This procedure allowed the preparation of the soil at the desired moisture content value with a maximum error of ±0.5% in terms of absolute water content.

Steam was supplied at a relative pressure of 50 kPa with a flow rate of 0.6 kg/h for all the considered techniques. The operating temperature of the steam superheater was set at 120 °C to limit condensation in the pipes.

In each experiment steam supply phase was followed by a cooling phase, which was monitored for a period lasting two times than steam supply. In trials with injector or hood, the heating phase lasted 15 minutes. To reach comparable temperatures in the soil, on the basis of preliminary tests, the supplying phase for sheet steaming was set at 60 minutes.

3.5. *Measurement of the moisture profile*

In order to locate the condensation front caused by superficial steam application and the portion of soil bulk interested by biphasic flux during steam injection, moisture profiles after the treatment were determined for the three steam application techniques in separate trials at the same conditions of the previous experimentations, that is on the two soils, at three initial water content level.

The procedure described in Hochstein & Bromley (2005) was adopted, analysing a set of core samples in a vertical section of soil. To collect the samples, an appropriate wood box (380 mm x 380 mm x 340 mm) was built and equipped with a drilled steel blade, which allowed the soil bulk vertical sectioning just after the end of steam supply. The removal of the soil from one side of the blade, allowed the sampling of the cores, which were taken with a small (15 mm diameter and 30 mm length) core sampler through the blade holes. The 63 holes (16 mm diameter and 30 mm spaced) were drilled in the steel blade according to a 7 x 9 matrix, with exception of the first two lines on the top that were 20 mm spaced. The blade allowed collecting samples in an area of 300x200 mm.

During the trials the hood was placed on the surface at the centre of the box while the injector was buried at a distance of 1 cm from the border of the box with the supplying hole at 12 cm depth and the flux direction laying on the plane of the blade. Moisture content was expressed according to Eq.1.

3.6. *Statistical analysis*

To evaluate the effect of soil features, specifically texture and water content, on heating efficiency, we introduced the scalar index

$$I(T) = \frac{1}{t_f V} \int_0^{t_f} \int_0^{x_V} \int_0^{y_V} \int_0^{z_V} T(t;x,y,z) - T(t;x,y,z)\, dz\, dy\, dx\, dt \qquad \forall (x,y,z) \in V \tag{2}$$

to represent the cumulative effect of the treatment on the trial volume of soil during the test. $I(T)$ represents the average of the temperature increases (calculated as the differences from the initial soil temperature $T(0;x,y,z)$), on the trial volume V of coordinates $(0,x_V)$, $(0,y_V)$ and $(0,z_V)$, during the test lasting from $t=0$ to $t=t_f$. Index was numerically calculated using the data collected at the sampling instants from the 48 probes of the measuring system. The index $I(T)$ is independent of the initial soil temperature, in the range taken into account, and compensates the different acquisition durations for the sheet steaming techniques (180 minutes) and hood and injector (45 minutes). The index has allowed for assessment of the efficiency of soil heating for the considered techniques as well as an evaluation of the dependency on the soil features.

The performance index was calculated for each of the 54 trials scheduled by the experimental plan. Data were subjected to variance analysis taking into account the steam distribution systems (sheet steaming, hood and injector), the soil type (Soil A and Soil B) and the moisture content levels (40%, 60% and 80% of FC). To this extent a three ways full factorial model ANOVA was adopted. Means were separated by a post hoc Bonferroni test, on a SPSS 13® platform.

4. Results

Temperature data and moisture profiles were analyzed in two subsequent steps. Firstly, a comparison of the three steam application systems was carried out evaluating the behaviour of soil temperature during and after steam application. Afterwards, the effect of soil texture and water content on heating efficiency was evaluated. Finally, moisture profiles and temperature data are used to discuss the results obtained at different soil conditions.

4.1. *Comparison* of *steam distribution systems.*

In Fig. 3 and 4 the 3D spatial distributions of the temperature of the soil A plotted for nine subsequent time instants for hood and injector treatments are demonstrated. Data refer to the three depths of the probe grid as well as to 12 cm of depth, which corresponds to the depth

of the steam supply by the injector. In Fig. 5 and 6 each curve shows the average temperature of the soil sampled by the 16 thermocouples placed on the same grid.

Temperature time-space distributions gave a detailed spatial description of soil heating with the different techniques (Fig. 3 and 4) and explain the dominant physical dynamics driving the soil heating of the layers at different depths (Fig. 5 and 6). During the steam-supplying phase, when heating is due to the flow and condensation of the steam, the average temperature curve slope is very steep, instead when it is a consequence of thermal conduction it's smoother.

The heating dynamics forced by the two surface steam distribution techniques (sheet steaming and hood) showed a similar behaviour, but with higher heating rates for the hood (Fig. 3).

As shown in Fig. 5, sheet steaming heating dynamics are very slow and, in spite of 60 minutes of steam supply, only the upper layer reached adequate temperatures for disinfestation at all moisture conditions. Lower layers are heated very slowly, denoting the prevailing thermal conduction. In the middle layer (9 cm), heating proved to be strongly dependent on the water content of the soil. Moreover, it is important to notice that heating in the lower layers continued after the steam supply ended, due to heat transfer from the upper layers (Dabbene et al., 2003).

In the case of the hood steamer, as can be seen in the sequence of Fig. 3, the higher layer (3 cm depth) reaches a uniform temperature of about 100°C in a few minutes because it is fully filled by the steam flow. The pressure coerced under the iron hood forces a mass transport phenomenon, which involves also the layer at the 9 cm depth after a short time delay which the duration resulted to be higher in the case of dryer soil (Fig. 6, on the left). Nevertheless the heating of the deepest layer (15 cm) is negligible. This behaviour can also be noted analyzing the curves of average temperatures at increasing depths and the transient decrease of their slope. The curves concerning the deepest layer (red lines) denote that here thermal conduction is the dominant heat transfer mechanism. Similar results were obtained by Pinel et al. (2000) in a set of field trials of a self-propelled machine equipped with metal hoods.

The steam injection technique (Fig. 4) gave the best results in terms of efficiency and homogeneity of heating. Steam, injected into the soil at 12 cm depth, flows towards the upper layers, quickly heating the layer at the 9 cm depth and then the entire soil bulk. The

obtained temperature is fairly homogeneous in the whole soil volume. Fig. 6, on the right, shows how, even in the worst case (i.e. Soil A at 40% of FC), a mean temperature of 60°C is reached in all layers at the end of steam supply phase. The quick rise of the average temperature curves, in fact, shows that all layers are directly affected by the steam flow. Furthermore, also the deepest layer of soil follows a similar curve, although it is about 3 cm below the steam application point.

Results on time-space temperature distribution conducted on soil B by the three techniques, presented behaviour similar to those obtained on soil A (data not reported).

The effect of the different soil texture and moisture content of the two used soils will be more thoroughly discussed in the next paragraph.

4.2. *Effect of soil texture and moisture content on heating efficiency*

Performance indexes resulted to be significantly different for the factors distribution technique and moisture content, whereas soil type did not significantly affect the index (Table 3). Significant differences were found among all three steam distribution techniques, as well as among all three considered soil moisture levels as resulted from the Bonferroni test (not reported).

Concerning the two way interactions, significant differences were identified concerning Soil-Moisture and Technique-Moisture, whereas no statistical differences were seen concerning Technique-Soil as well as for the three ways interaction.

The best performances were obtained with the sub-surface steam injection followed by hood and sheet steaming, in the whole range of considered moisture levels (Fig. 7). Performance index for the sandy-loam soil (soil A) is more intensively influenced by moisture than sandy soil (soil B), as shown by the significant difference related to Soil-Moisture interaction.

Furthermore, the effect on soil heating with respect to moisture levels is different for the three steam application techniques. For sheet steaming, performance indexes increased for both soils at higher moisture contents, achieving higher heating efficacy. This is the same for all depths tested (Fig. 5), where the average temperatures measured by the probe at increasing depths for Soil A at 40% of FC are significantly lower than the ones measured at 80% of FC. Only at higher moisture content the deepest layer reaches a temperature close to 60°C, and the temperature of the intermediate layer rapidly increased, reaching a maximum

value of about 85°C. The sheet steaming treatment for this soil reached an adequate degree of disinfestation only at 80% of FC.

With regard to the hood, in the case of Soil A, a linear relationship between moisture content and the performance index was observed. On the contrary, in Soil B the effect of moisture content results negligible. This can be seen in the temperature graphs of Fig. 6 (soil A) and Fig. 8 (soil B). In particular, for Soil B, the difference among the average temperature curves concerning the highest and the lowest moisture levels are almost unnoticeable. In the case of Soil A, instead, considerable difference can be observed between the cases at the two water content values, especially in the intermediate layer which was affected by steam only at 80% FC. This behaviour is confirmed by moisture profiles of Fig. 9. In Soil A at 40% of FC, the region with the highest moisture content, at the end of the steam supplying phase, is located close by the surface (up to 5 cm depth), whereas at 80% of FC it is positioned at a depth ranging from 5 to 16 cm. Higher water content (Fig. 9) indicates the presence of the condensation front that typically moves towards the deepest layers increasing soil moisture as indicated by temperature data. Concerning Soil B, the shift downwards of the moist region resulted to be negligible (Fig. 9), which indicates that this region was reached only by a small amount of steam. Furthermore, the steam flux does not reach the layers beyond 13 cm depth, where no moisture increase was detected with respect to the initial value, according to temperature data. However, it has to be noted that at 40% of FC and for both types of soil, the condensation front is located near the surface, whereas at 80% of FC it is formed in a deeper layer. At 80% of FC, a lower moisture content in the top layer (2 cm depth) was observed, even if this layer of soil is directly reached by the steam supplied by the hood. This phenomenon argues the presence of the upstream region discussed in Section 2.

In the case of the injector, performance indexes have a positive trend in function of moisture content in Soil A, whereas a maximum was observed in Soil B, at a moisture content of 60% of FC (Fig. 7). In Soil A, the soil was more easily heated at each depth at a moisture content of 80% of FC in comparison with drier soil at 40% of FC also in the case of steam injection (Fig. 6 on the right).

As could be seen from Fig. 10, after injection in Soil B, in the case of 80% of FC soil, the steam expands and condenses in a wider portion of the soil, enhancing moisture level more

than in the case of the 40% FC soil. Biphasic flux also involves the layers below the steam application point up to 19 cm (Fig. 10), independently of initial soil water content.
The moisture patterns obtained with the injector also show that steam does not exceed a maximum horizontal distance of 15 cm from the injection point. This distance has to be taken in account when designing a system of multiple sub-surface injectors, in particular concerning the distance from adjacent injectors.

The results obtained showed an overall increase of the heating efficiency with the soil water content, even if the reliance on moisture is higher in sandy-loam soil (Soil A) than in sandy soil (Soil B). In general, thermal conductivity and diffusivity of soil, as well as its heat storage capacity, increase with water content (Abu-Hamdeh, 2001, Balghouthi et al., 2005). However, the different behaviour in the two soil types can be attributed to their texture, in particular to the presence of a greater percentage of silt and clay in Soil A.
Thermal diffusivity in sandy-loam soil, similar to Soil A, was studied by Usowicz et al. (1996). This parameter resulted in increases with water content, achieving a maximum for moisture close by FC. For sheet steaming similar behaviour was obtained on-field by Minuto et al. (2005), who found the maximum heating efficiency on sandy-loam soil at the moisture range corresponding about to 80% of FC in present work.
Performance indexes at the lowest considered moisture contents are considerable lower in Soil A than in Soil B for all steam distribution equipments. This behaviour might be explained by the greater water retention capacity of sandy-loam soil with respect to a sandy soil. The higher percentage of silt and clay in Soil A turns out in an increase of the cohesion forces among water and soil particles owing to their relatively small dimensions. When soil is rather dry, therefore, liquid and vapour phase diffusion due to temperature and moisture gradients is less intense than in wet soil (Philip & De Vries, 1957). As denoted by moisture profiles of Fig. 9 and Fig. 10, an increase of the moisture content results in a more intense mass transfer regarding, in particular, the liquid phase diffusion (Philip & De Vries, 1957).
Sandy soils are considered more difficult to steam than sandy-loam soils due to their dense structure (Minuto et al., 2005; Runia, 1983). Performance indexes of Fig. 7 show that, in Soil B, the maximum heating efficiency is achieved at a moisture degree lower than in Soil A. Furthermore, performance indexes calculated for Soil B are always lower with respect to

Soil A at the highest value of water content for all the considered steam application systems, according to Minuto et al. (2005).

5. Conclusions

The effects of different steam application systems for soil disinfestation have been presented in this paper. The equipment design followed an extensive laboratory experimentation phase during which two surface steam distribution techniques (sheet steaming and metal hoods) were compared to sub-surface steam injection.

It was demonstrated how soil water content, as well as texture, influence the soil heating efficiency for the compared steam distribution techniques. Levels of moisture close to the field capacity gave, in general, high value of heating efficiency, even if the reliance on the moisture is higher in sandy-loam soil than in sandy soil. The maximum values of performance index have been found at 80% of FC in sandy-loam soil for all the compared techniques, while lower maximum values have been obtained in sandy soil.

Although physical soil properties cannot be modified in real field conditions, except for moisture content controlled by irrigation, it is important to understand their influence upon the efficiency of soil heating, in order to regulate the duration of the steam application in the best and most effective way.

Acknowledgements

Authors would like to thank Fernando De Palo for his help during the experimental phase.

This work was partially supported by the grants of Assessorato per l'Agricoltura of the Regione Piemonte, Italy.

References

Abu-Hamdeh N H (2001). Measurement of the thermal conductivity of sandy loam and clay loam soils using single and dual probes. J. Agric. Engng Res., **80**(2), 209-216, doi:10.1006/jaer.2001.0730

Balghouthi M; Kooli S; Farhat A; Daghari H; Belgith A (2005). Experimental investigation of thermal and moisture behaviours of wet and dry soils with buried capillary heating system. Solar Energy, **79**, 669-681

Bartok J W Jr (1994). Steam sterilization of growing media. Proceeding of: Forest and Conservation Nursery Associations, Williamsburg, VA, 11-14 July

Bergins C; Crone S; Strauss K (2005). Multiphase flow in porous media with phase change. Part II: analytical solutions and experimental verification for constant pressure steam injection. Transport in porous media, **60**, 275-300, doi 10.1007/s11242-004-5740-5

Brouwers H J H (1996). An experimental study of constant-pressure steam injection and transient condensing flow in an air-saturated porous medium. Journal of Heat Transfer, **118**, 449-454, doi:10.1115/1.2825865

Cavazza L (1981). Fisica del terreno agrario. UTET (in italian).

Crone S; Bergins C; Strauss K (2002). Multiphase flow in homogeneous porous media with phase change. Part I: Numerical modelling. Transport in porous media, **49**, 291-312, doi:10.1023/A:1016271213503

Dabbene F; Gay P; Tortia C (2003). Modeling and control of steam soil disinfestation processes. Biosystems Engineering, **84**, 3, 247-256, doi:10.1016/S1537-5110(02)00276-3

Egli M; Mirabella A; Kägi B; Tomasone R; Colorio G (2006). Influence of steam sterilisation on soil chemical characteristics, trace metals and clay mineralogy. Geoderma, **131**, 123-142, doi:10.1016/j.geoderma.2005.03.017

Fenoglio S; Gay P; Malacarne G; Cucco M (2006). Rapid recolonisation of agricultural soil by microarthropods after steam disinfestation. Sustainable Agriculture, **27** (4), 125-135, doi:10.1300/J064v27n04-09.

Gay P; Piccarolo P; Ricauda Aimonino D; Tortia C (2008). Soil parameter effects on steam disinfestation efficiency. AgEng 2008 - International Conference on Agricultural Engineering - Conference Proceedings CD, Hersonissos, Crete, Greece. 23-25 June 2008

Gay P; Piccarolo P; Ricauda Aimonino D; Tortia C (2010). A high efficacy steam soil disinfestation system, Part II: Design and Testing. Submitted to Biosystems Engineering.

Gilbert C; Fennimore S; Subbarao K; Hanson B; Rainbolt C; Goodhue R; Ben Weber J; Samtani J (2009). Systems to disinfest soil with heat for strawberry and flore production. MBAO 2009 - Annual International Research Conference on Methyl Bromide Alternatives and Emissions Reductions – Conference proceeding, San Diego, California, USA. 10-13 November 2009.

Hanamura K; Kaviany M (1995). Propagation of condensation front in steam injection into dry porous media. Int. J. Heat Mass Transfer, **38**, 1377-1386

Hochstein M P; Bromley C J (2005). Measurement of heat flux from steaming ground. Geothermics, **34**, 133-160, doi:10.1016/j.geothermics.2004.04.002

Iwamura K; Kaneshima S (2005). Numerical simulation of the steam-water instability as a mechanism of long-period ground vibrations at geothermal areas. Geophysical Journal International, **163**, 2, 833-851, doi: 10.1111/j.1365-246X.2005.02749.x

Lawrence W J C (1956). Soil Sterilization. Unwin Brothers Limited, London

Miller C T; Christakos G; Imhoff P T; McBride J F; Pedit J A (1998). Multiphase flow and transport modelling in heterogeneous porous media: challenges and approaches. Advances in Water Resources, **21**, 77-120, doi:10.1016/S0309-1708(96)00036-X

Minuto G; Gilardi G; Kejji S; Gullino M L; Garibaldi A (2005). Effect of physical nature of soil and humidity on stream disinfestation. Acta Horticulturae, **698**, 257-262

Nederpel L (1979). Soil disinfestation. Mulder D (Editor) Elsevier Scientific Publishing Company, Amsterdam

Philip J R; De Vries DA (1957). Moisture movement in porous materials under temperature gradients. Transactions of American Geophysical Union, **38** (2), 222-232

Pinel M P C; Bond W; White J G (2000). Control of soil-borne pathogens and weeds in leaf salad monoculture by use of a self-propelled soil-steaming machine. Acta Horticulturae, **532**, 125-130

Ricauda Aimonino D (2008). Tecniche e strategie innovative ed eco-compatibili per la difesa delle colture ad alto reddito, PhD Thesis, Torino, Italy, (in italian)

Roux-Michollet D; Czarnes S; Adam B; Berry D; Commeaux C; Guillaumaud N; Le Roux X; Clays-Josserand A (2008). Effects of steam disinfestation on community structure, abundance and activity of heterotrophic, denitrifying and nitrifying bacteria in an organic farming soil. Soil Biology & Biochemistry, **40**, 1836-1845, doi:10.1016/j.soilbio.2008.03.007

Runia W T (1983). A recent development in steam sterilization. Acta Horticulturae, **152**, 195-200

Runia W T (2000). Steaming methods for soils and substrates. Acta Horticulturae, **532**, 115-123

Shoda A; Wang C Y; Cheng P (1998). Simulation of constant pressure steam injection in a porous medium. Int. Comm. Heat Mass Transfer, **26** (6), 753–762, doi:10.1016/S0735-1933(98)00062-1

Usowicz B; Kossowski J; Baranowski P (1996). Spatial variability of soil thermal properties in cultivated filed. Soil & Tillage Research, **39**, 85-100, doi:10.1016/S0167-1987(96)01038-0

Van Loenen M C A; Turbett Y; Mullins C E; Feilden N E H; Wilson M J; Leifert C; Seel W E (2003). Low temperature-short duration steaming of soil kills soil-borne pathogens, nematode pests and weed seeds. European Journal of Plant Pathology, **109**, 993-1002, doi:10.1023/B:EJPP.0000003830.49949.34

Wahba G (1990). Spline models for observational data, SIAM, Philadelphia

Tables

Table 1. Characteristics of the two soils used during the experimentation.

Soil	Sand %	Silt %	Clay %	Bulk Density kg m^{-3}	Field Capacity kg 100 kg^{-1}	Saturated water content kg 100 kg^{-1}
A	69.4	15.5	15.1	1.23	15.7	37.5
B	85.2	7.8	6.3	1.20	14.1	31.5

Table 2. Absolute values of considered water contents (percentage of dry soil weight) referred to the defined percentage of FC.

Percentage of FC, %	Absolute Moisture, kg 100 kg^{-1}	
	Soil A	Soil B
40	6.2	5.6
60	9.3	8.4
80	12.4	11.2

Table 3. Results of the three ways ANOVA test

Factors	Sum of Sq	df	Mean Sq	F	Sig. of F
Technique	8670.99	2	4335.47	1008.87	0.000*
Soil	0.45	1	0.45	0.10	0.748
Moisture	401.07	2	200.54	46.66	0.000*
Technique x Soil	19.57	2	9.78	2.28	0.117
Technique x Moisture	83.92	4	20.98	4.88	0.003*
Soil x Moisture	115.79	2	57.90	13.47	0.000*
Technique x Soil x Moisture	18.33	4	4.58	1.07	0.387
Error	154.70	36	4.30		

*Mean difference is significant at the 0.005 level

R squared=0.984 ; adjusted R squared=0.976)

Figures

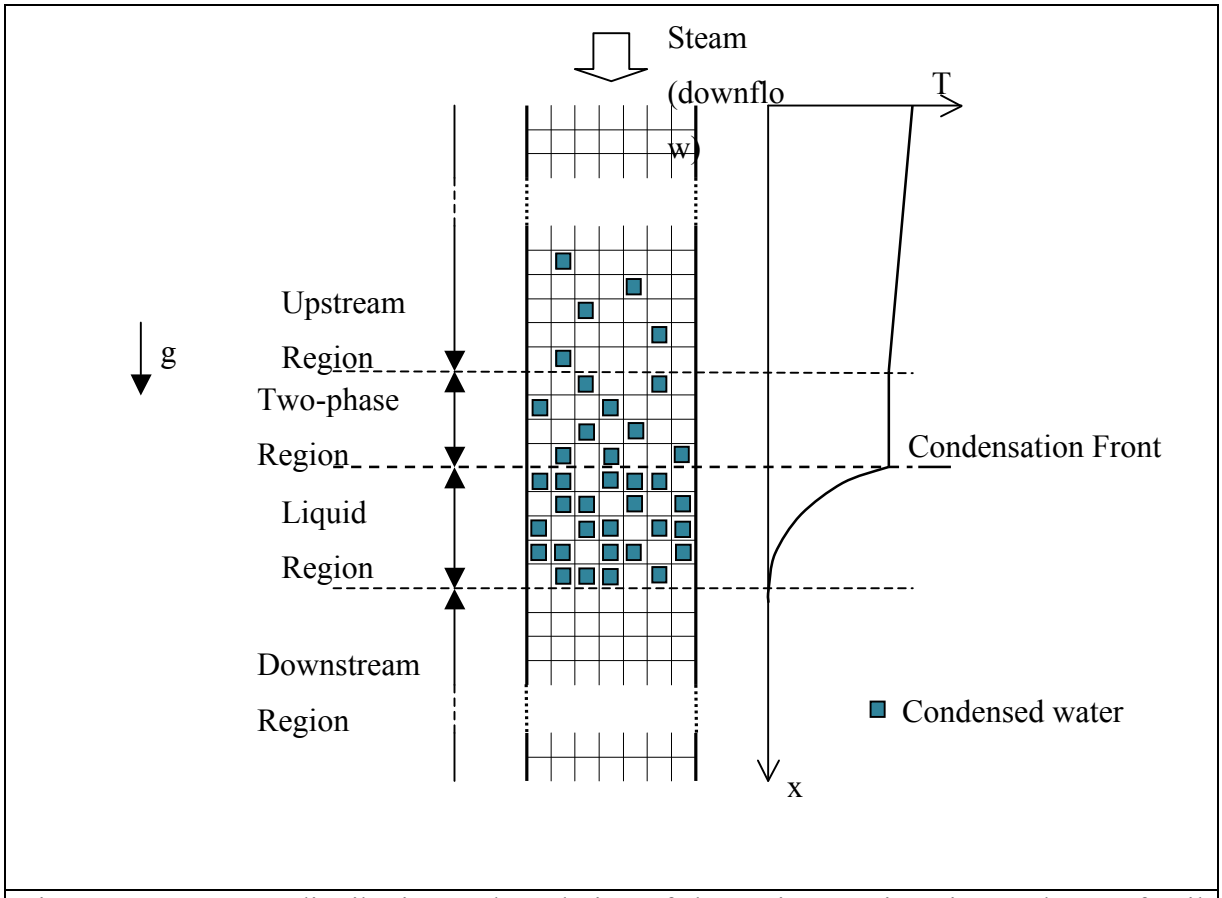

Fig. 1. Temperature distribution and rendering of the various regions in a column of soil during a steam treatment from the surface

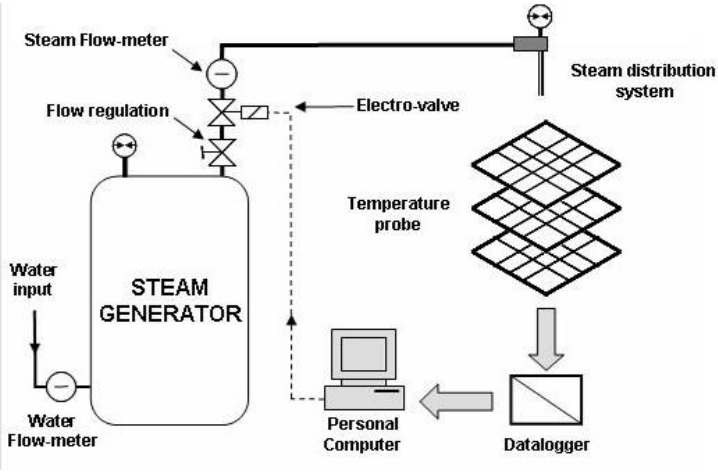

Fig. 2. Layout of the pilot plant used for the experimentation.

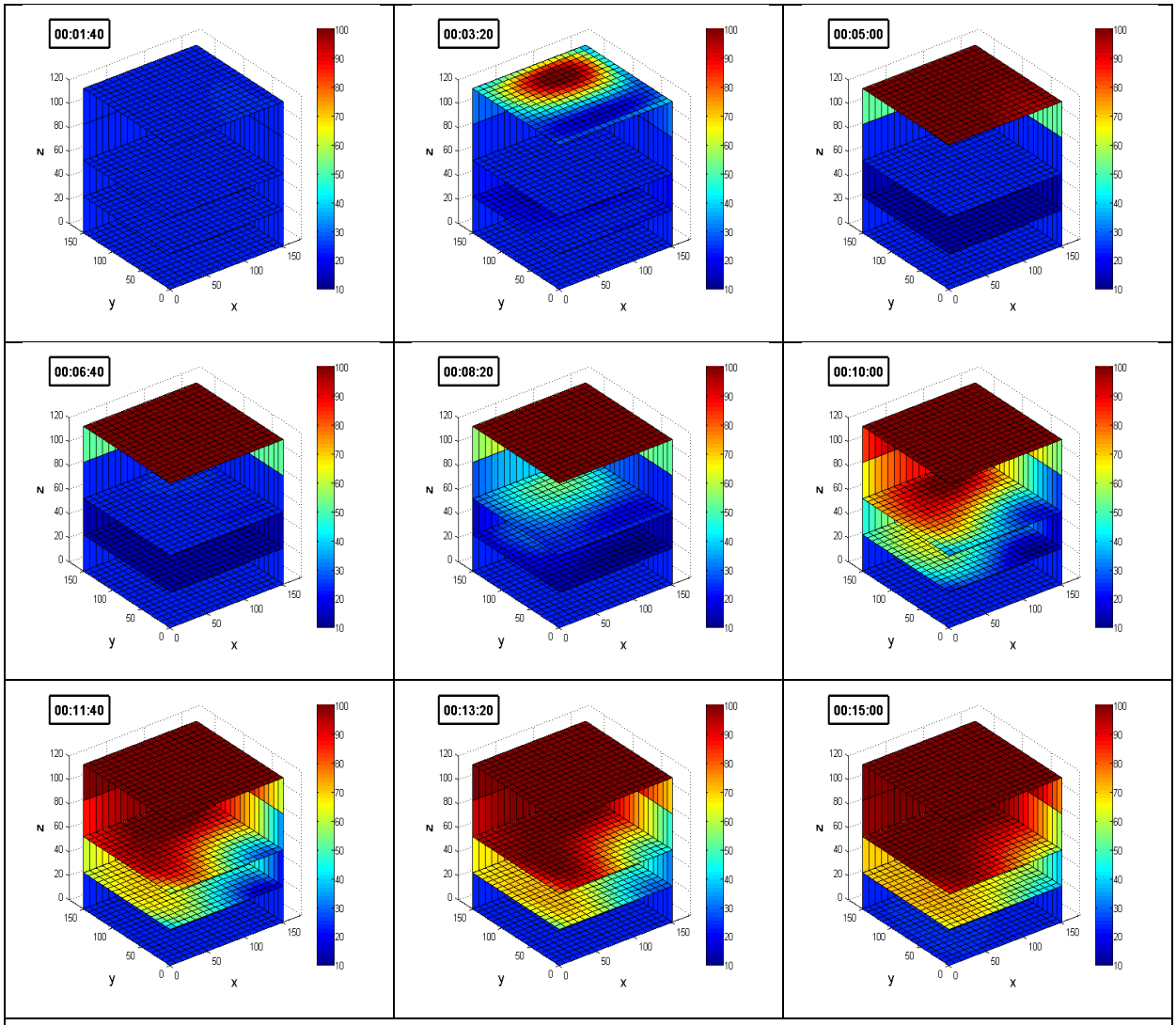

Fig. 3. Temperature spatial distribution in the soil A during the iron hood treatment, after 100, 200, 300, 400, 500, 600, 700, 800, 900 s (from the upper left to the bottom right). Axes scales are expressed in mm.

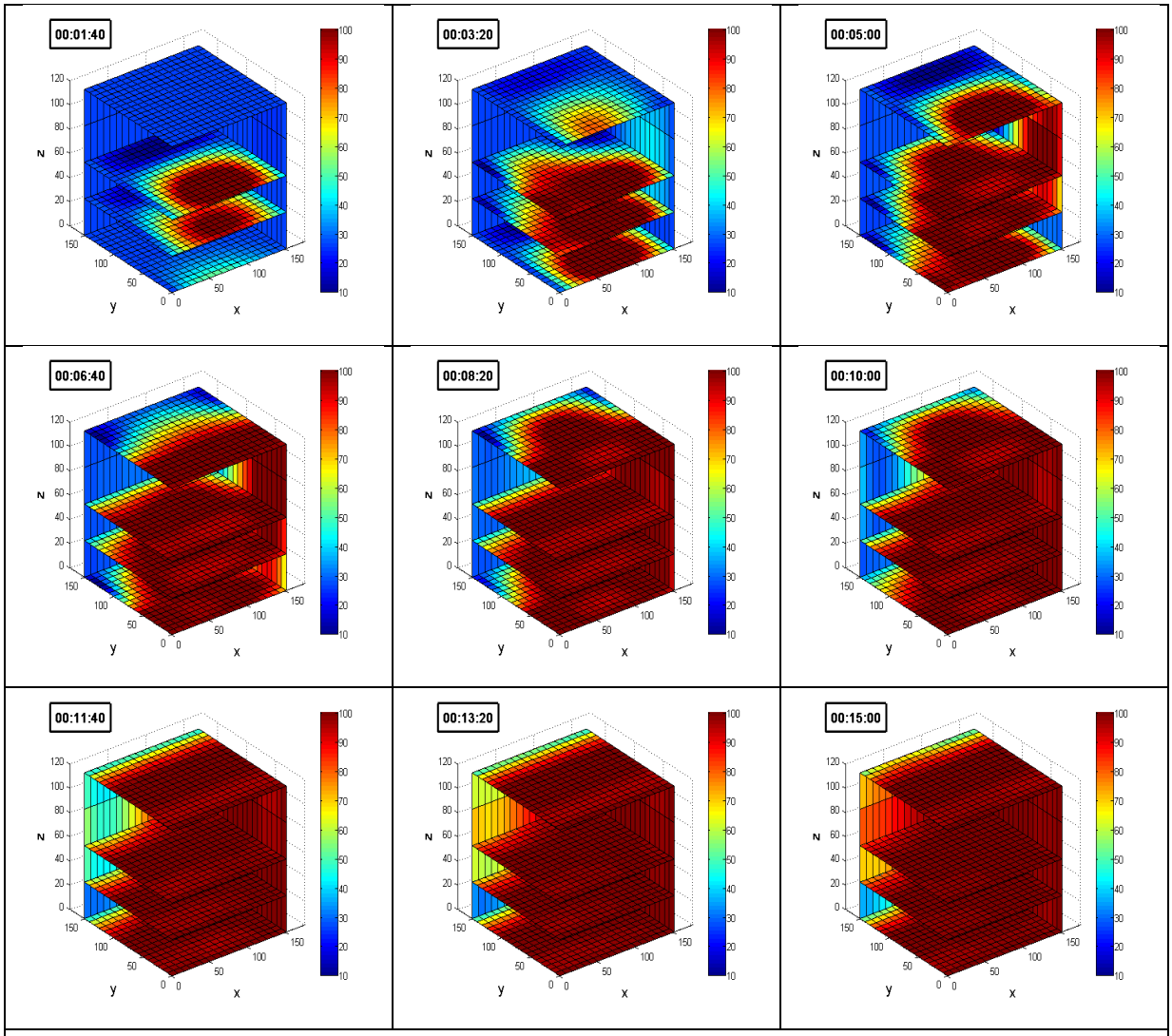

Fig. 4. Temperature spatial distribution in the soil A during the buried injector treatment, after 100, 200, 300, 400, 500, 600, 700, 800, 900 s (from the upper left to the bottom right). Axes scales are expressed in mm.

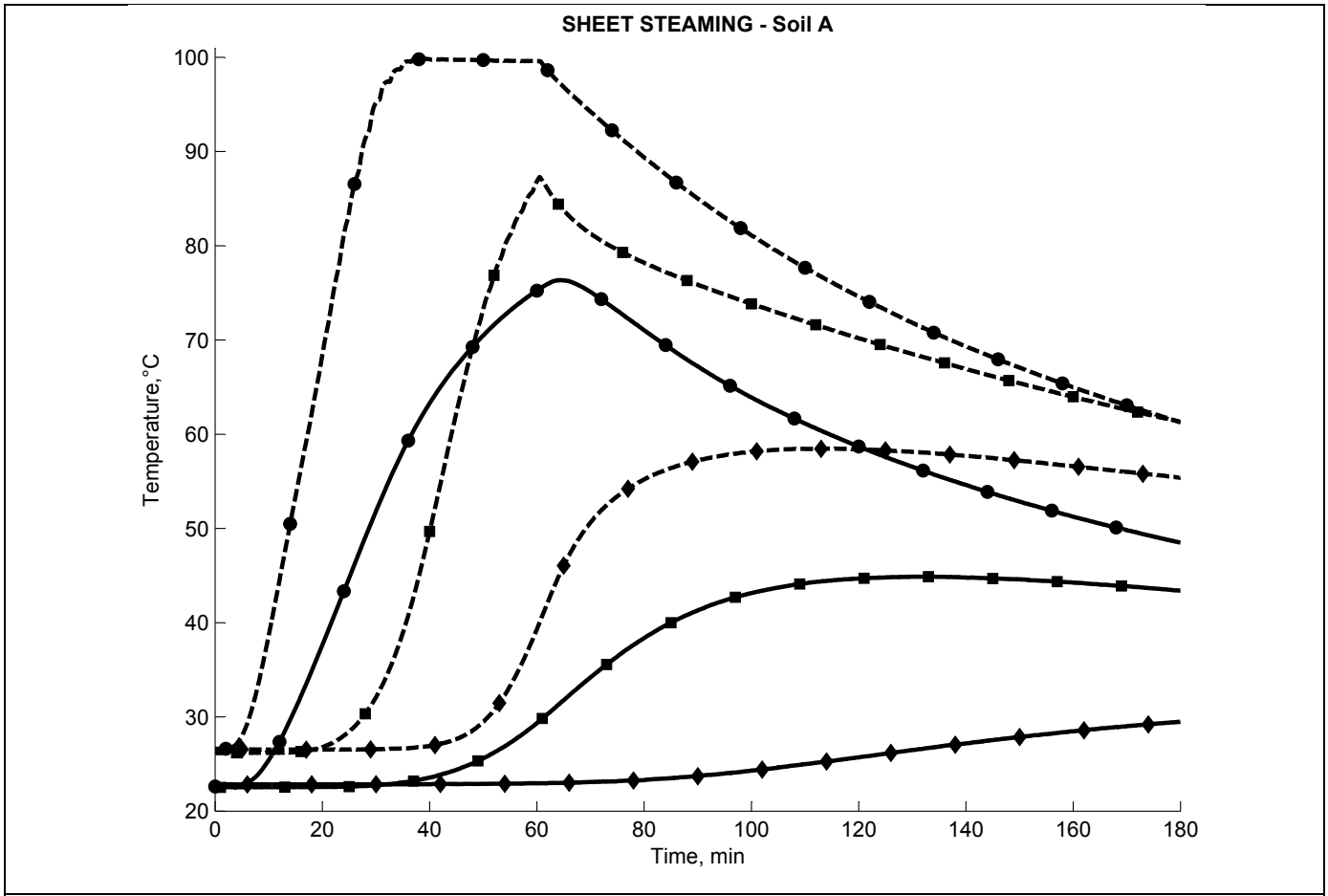

Fig. 5. Average temperatures measured at depth of 3 cm (●), 9 cm (■) and 15 cm (♦), for soil A, in the case of sheet steaming at different initial moisture: 40% of FC (———) and 80% of FC (- - -).

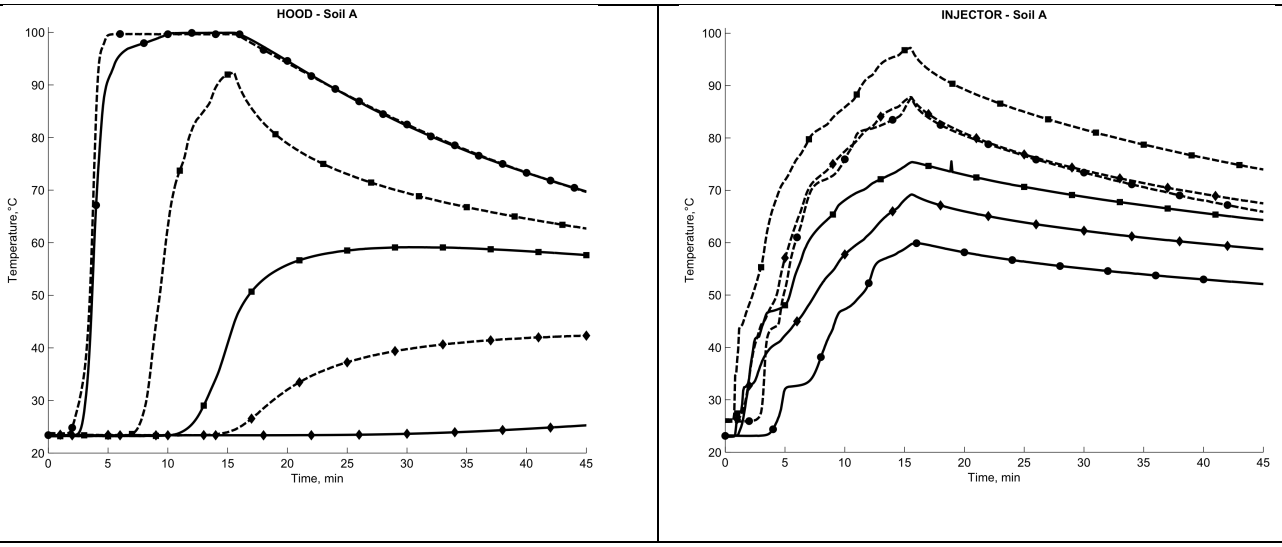

Fig. 6. Average temperatures measured at a depth of 3 cm (●), 9 cm (■) and 15 cm (♦), for soil A, at different initial moisture: 40% (——) and 80% (- - -) of FC; iron hood (on the left) and the buried injector (on the right) treatments.

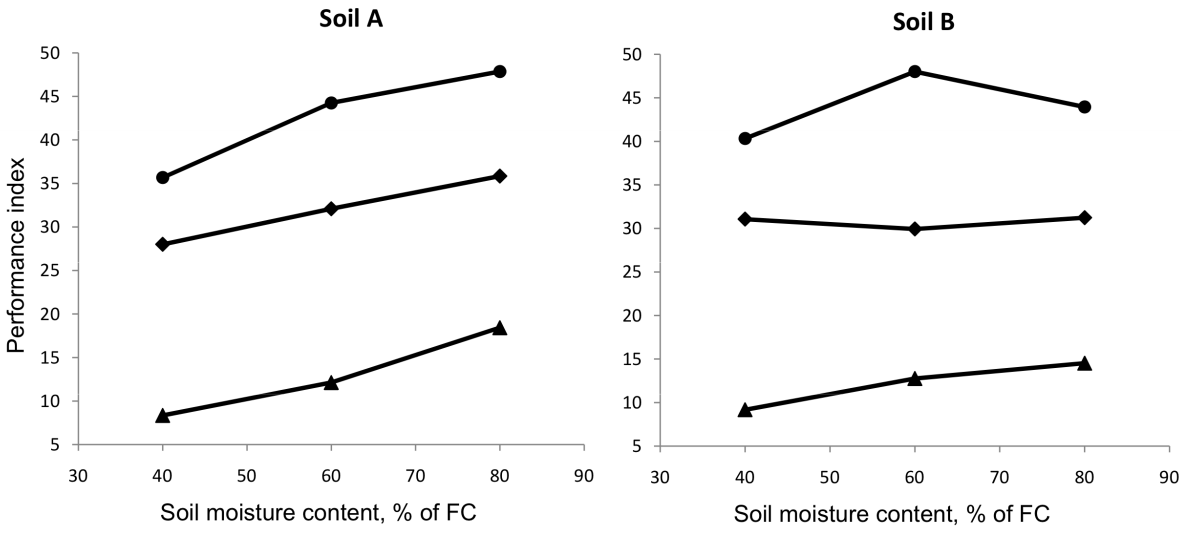

Fig. 7. Performance index vs soil moisture content for the soil A (on the left) and the soil B (on the right) in the case of hood (●), injector (♦) and sheet steaming (▲) treatments.

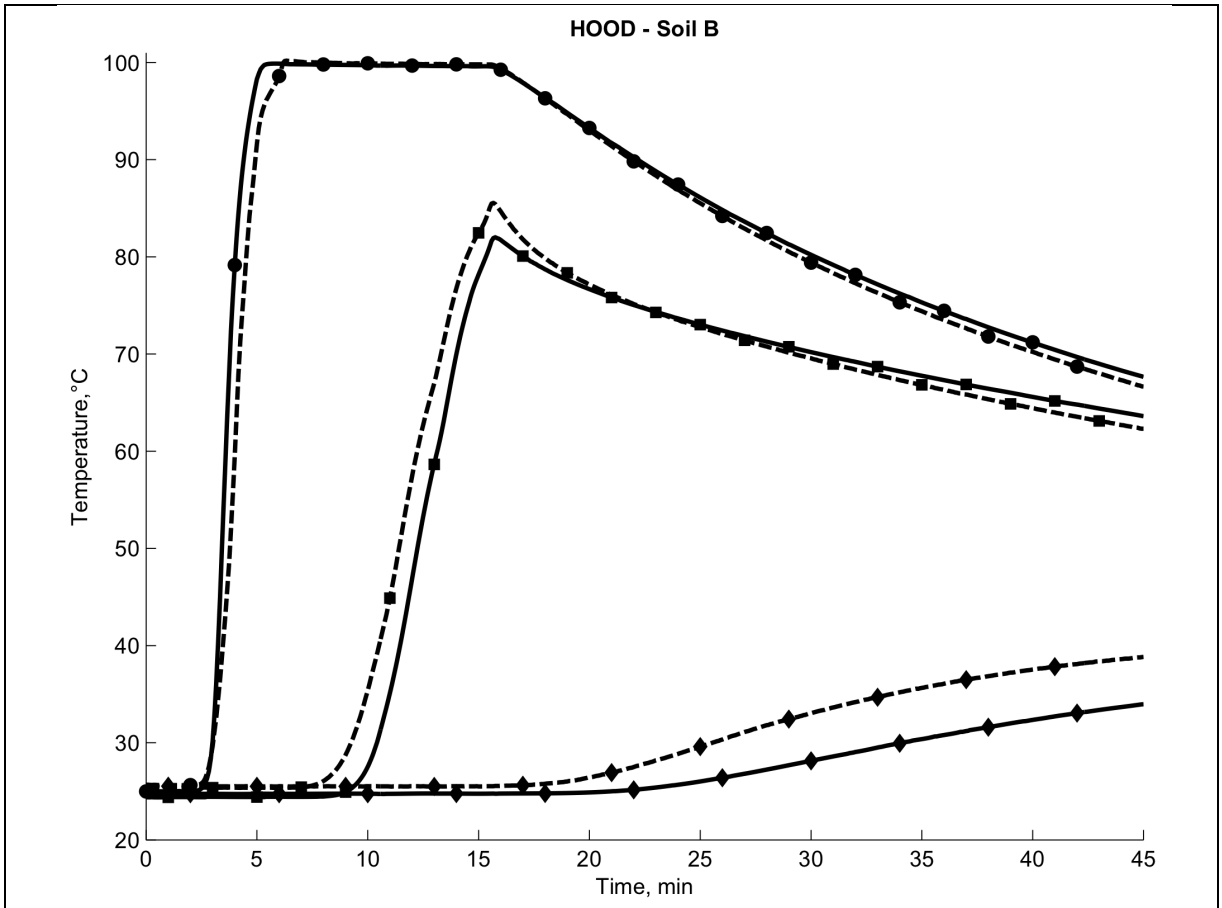

Fig. 8. Average temperatures measured at a depth of 3 cm (●), 9 cm (■) and 15 cm (♦), during trials with hood on soil B: comparison of the cases for humidity at 40% (——) and 80% (- - -) of FC.

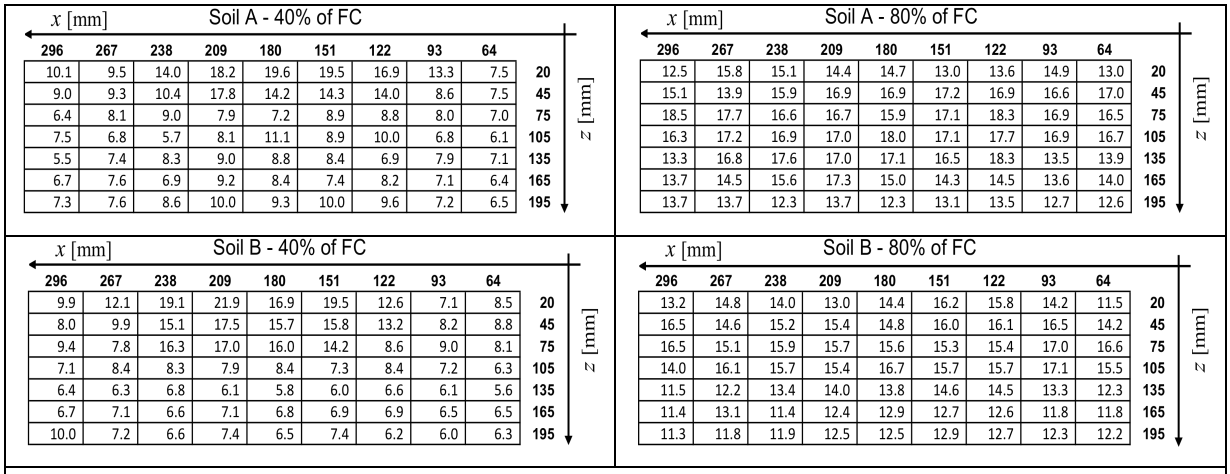

Fig. 9. Moisture profile of soil A (on the top) and soil B (on the bottom), in the case of 40% of FC (on the left) and 80% of FC (on the right) in trials with the iron hood. In each cell is reported the moisture content of the soil cores sampled by the blade. *x* coordinate reports the distance from the blade border while *z* coordinate is referred to the distance from soil the surface (mm).

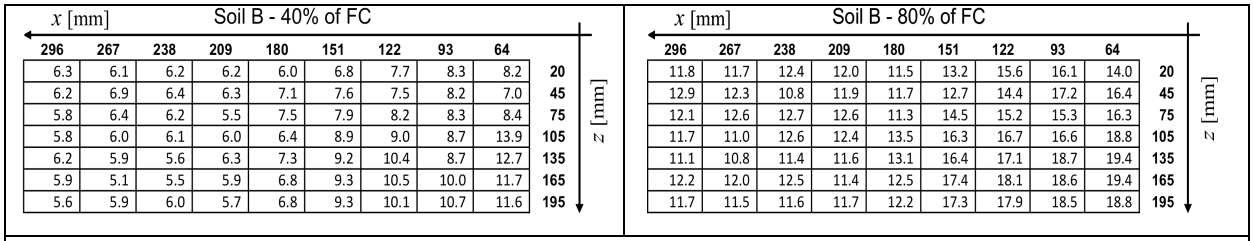

Fig. 10. Moisture profile of soil B in the case of 40% of FC (on the left) and 80% of FC (on the right) in trials with the steam injector, placed on the right. In each cell is reported the moisture content of the soil cores sampled by the blade. *x* coordinate reports the distance from the blade border while *z* is referred to the distance from the soil surface (mm).

List of captions

Fig. 1. Temperature distribution and rendering of the various regions in a column of soil during a steam treatment from the soil surface

Fig. 2. Layout of the pilot plant used for the experimentation

Fig. 3. Temperature spatial distribution in the soil A during the iron hood treatment, after 100, 200, 300, 400, 500, 600, 700, 800,900 s (from the upper left to the bottom right, respectively). Axes scales are expressed in mm.

Fig. 4. Temperature spatial distribution in the soil A during the buried injector treatment, after 100, 200, 300, 400, 500, 600, 700, 800,900 s (from the upper left to the bottom right, respectively); axes scales are expressed in mm.

Fig. 5. Average temperatures measured at a depth of 3 cm (●), 9 cm (■) and 15 cm (♦), for soil A, in the case of sheet steaming at different initial moisture: 40% of FC (———) and 80% of FC (- - -).

Fig. 6. Average temperatures measured at a depth of 3 cm (●), 9 cm (■) and 15 cm (♦), for soil A, at different initial moisture: 40% (———) and 80% (- - -) of FC; iron hood (on the left) and the buried injector (on the right) treatments.

Fig. 7. Performance index vs soil moisture content for the soil A (on the left) and the soil B (on the right) in the case of hood (●), injector (♦) and sheet steaming (▲) treatments.

Fig. 8. Average temperatures measured at a depth of 3 cm (●), 9 cm (■) and 15 cm (♦), during trials with hood on soil B: comparison of the cases for humidity at 40% (———) and 80% (- - -) of FC.

Fig. 9. Moisture profile of soil A (on the top) and soil B (on the bottom), in the case of 40% of FC (on the left) and 80% of FC (on the right) in trials with the iron hood. In each cell is

reported the moisture content of the soil cores sampled by the blade. *x* coordinate reports the distance from the blade border while *z* coordinate is referred to the distance from soil the surface (mm).

Fig. 10. Moisture profile of soil B in the case of 40% of FC (on the left) and 80% of FC (on the right) in trials with the steam injector, placed on the right. In each cell is reported the moisture content of the soil cores sampled by the blade. *x* coordinate reports the distance from the blade border while *z* is referred to the distance from the soil surface (mm).

Notation table

Parameter	**Meaning**
M	Soil water content (%)
m_w	Mass of wet soil (kg)
m_d	Mass of dry soil (kg)
$T(t;x,y,z)$	Temperature of the soil at time instant t, at position (x,y,z)
V	Soil volume
t	Time variable
t_f	Treatment duration
(x,y,z)	Spatial coordinates
(x_V,y_V,z_V)	Dimensions of the trial volume of soil under study
$I(T)$	Index representing the average temperature increase on trial volume V